DESIGN OF FOUR-WHEEL INDEPENDENT DRIVE EV DIRECT YAW MOMENT CONTROLLER BASED ON DSPACE

Chuanwei ZHANG[1,2], Rui WANG[1,*], Dongsheng ZHANG[1], Rongbo ZHANG[1], Suzhe YUAN[2,3]

In order to improve the stability of four-wheel independent drive electric vehicle under direct yaw moment control, a hierarchical structure yaw moment controller is designed. The upper controller adopts fuzzy PID algorithm to solve the yaw moment. The lower controller takes the minimum tire utilization rate as the optimization objective and distributes the desired yaw moment calculated from the upper controller to each hub motor under the constraint of the adhesion of the motor and the road surface. dSPACE is used to carry out the hardware-in-the-loop experiment, and the results showed that the hardware-in-the-loop experiments are basically consistent with the simulation, the upper controller can well track the vehicle target motion state parameters, and the lower controller can better follow the reference state, reduce the tire utilization rate, and improve the stability of the vehicle.

Keywords: Electric vehicle; Direct yaw moment; Hardware-in-the-loop; Stability

1. Introduction

As an ideal carrier for researching vehicle control technology, the four-wheel independent drive electric vehicle greatly improves the transmission efficiency and controllable degrees of freedom. It is easier to achieve the direct yaw moment control of the vehicle by coordinating and controlling the output driving force of each hub motor, so as to achieve stable driving [1,2,3].

The existing direct yaw-moment control structure generally adopts a hierarchical form: the upper layer is the vehicle state tracking layer and according to the input of the driver and the current actual state information of the vehicle, the additional yaw-moment required for tracking the ideal state value under the premise of maintaining the stability of the vehicle is calculated; the lower layer is the distribution control layer, and the additional yaw moment obtained from the upper controller is distributed to each wheel in the form of driving force to change the motion state of the vehicle [4]. Among them, the researchers have used the

[1]College of Mechanical Engineering, Xi'an University of Science and Technology, Xi'an 710054, P.R. China.
[2]Shaanxi Key Laboratory of Integrated and Intelligent Navigation, Xi'an 710054, P.R. China.
[3]The 20th Research Institute of China Electronics Technology Corporation, Xi'an 710054, P.R. China.
*Rui WANG, Email:1214111936@qq.com

control method of modern control theory such as sliding mode control [5], fuzzy control [6,7,8], model predictive control [9,10]and generalized predictive control algorithm [11] for the design of the upper controller. The lower layer distribution controller currently uses more optimization algorithms [12,13], and the established objective function focuses on different aspects, such as the average working efficiency of economical motor [14,15]and the utilization adhesion rate of tire [16,17,18].

In this paper, a fuzzy PID controller that combined feedback yaw rate deviation is introduced to solve the additional yaw moment to improve the adaptive ability and robustness of the upper controller On this occasion, the minimum utilization rate of tire is taken as the optimization objective, and the adhesion force of motor and road surface is introduced as the constraint. Finally, the validity of the hierarchical controller is verified based on simulation test and hardware-in-loop test.

2. DYC Controller.

2.1 DYC Controller Structure

The controller structure is shown in Fig. 1. During the steering process, the driver expects the vehicle to have a linear response. Select the 2-dof model with lateral and yaw motion, based on this, the yaw rateγ_d is calculated by combining the steering wheel angle δ_s and the longitudinal speed V_X;The yaw moment calculator takes the difference between the expected yaw rate γ_d and the actual yaw rate γ , the rate of change of the difference as the input, and uses the fuzzy PID composite control algorithm to output the desired additional yaw moment ΔM; The yaw moment distributor distributes the generalized yaw moment to each hubmotor to control the yaw motion of the vehicle.

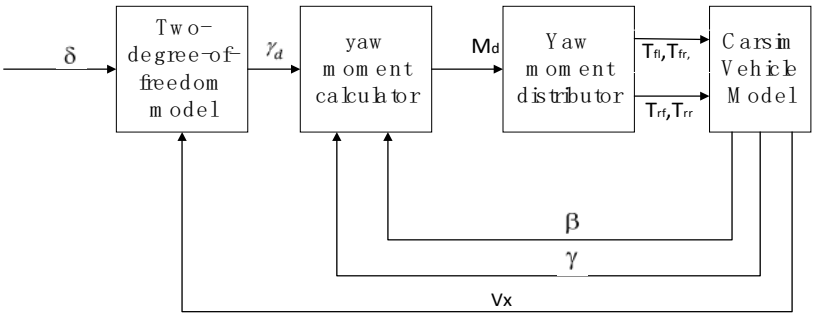

Fig. 1 Controller Structure

The linear 2-dof vehicle model is selected as the reference model:

$$\mathrm{m}(\dot{v}+\mu)=\left(C_f+C_r\right)\beta+\frac{1}{\mu}\left(aC_f-bC_f\right)-C_f\delta \tag{1}$$

$$J_z\dot{\gamma}=\left(\mathrm{a}C_f-bC_r\right)\beta+\frac{1}{\mu}\left(a^2C_f+b^2C_r\right)\gamma-aC_f\delta) \tag{2}$$

At steady state, the yaw rate is a fixed value [19].That is to say $\dot{\mathrm{v}}=0,\dot{\gamma}=0$,through calculation, yaw rate of the steady state value is:

$$\gamma_d=\frac{u/L}{1+Ku^2}\delta \tag{3}$$

Where, K—stability coefficient, $\mathrm{K}=\frac{\mathrm{m}}{\mathrm{L}^2}\left(\frac{\mathrm{a}}{\mathrm{C_r}}-\frac{\mathrm{b}}{\mathrm{C_f}}\right)$;L is the wheelbase between the front and rear axles. $\mathrm{C_r}$and $\mathrm{C_f}$is the lateral stiffness of the rear axle and front axle. a and *b* represent the distance from centroid to the front axle and rear axle; *u* is the longitudinal vehicle speed; μ represent the road adhesion coefficient; J_z is the moment of inertia around the z-axis.

2.2 Fuzzy PID Controller

In the process of driving on complex roads and steering of vehicles, the defects of fuzzy control that are not highly accurate are particularly prominent. The fuzzy PID controller is composed of fuzzy control and PID control, which can achieve high accuracy and strong online parameter self-tuning ability. The structure of the fuzzy PID controller is shown in figure 2:

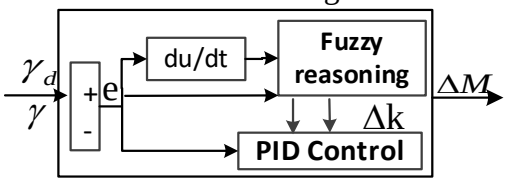

Fig. 2. Fuzzy PID composite control structure block diagram

The difference e between the expected yaw rate γ_{d} and the actual yaw rateγ, the rate of change of the difference ec,are taken as the input language variables of the fuzzy controller,$\mathrm{K_p}$, $\mathrm{K_i}$ and $\mathrm{K_d}$ are output language variables. Their range of variation is [-6,6] and [-1,1] respectively. The membership functions are all gaussian functions. Mamdani model is used to build fuzzy rules, and fuzzy rule reasoning is carried out for the yaw rate error e and its change rate ecafter fuzzy transformation, finally reasonable fuzzy PID control parameters are obtained. The final output of the composite controller is the additional yaw momentΔM.Specific fuzzy control rules of yaw rate are shown in Table 1 below:

Table 1

Fuzzy control rules of yaw rate

ec / e	NB	NM	NS	ZO	PS	PM	PB
NB	PB/ZO/PS	PS/PS/NS	PS/PS/NB	PS/PS/NB	PS/PS/NM	PS/PS/NM	PB/ZO/PS
NM	PB/ZO/PS	PS/PS/NS	PM/PM/NB	PS/PS/NM	PS/PS/NS	PS/PS/NS	PB/ZO/ZO
NS	PB/ZO/PS	PM/PS/NS	PS/PS/NM	PS/PS/NM	PS/PS/NS	PS/PS/NS	PB/ZO/ZO
ZO	PB/ZO/ZO	PB/PB/NS	PB/PB/NS	PS/PS/NS	PB/PB/NS	PB/PB/NS	PB/ZO/ZO
PS	PB/ZO/ZO	PS/PS/ZO	PS/PS/ZO	PS/PS/ZO	PS/PS/ZO	PM/PS/ZO	PB/ZO/ZO
PM	PB/ZO/ZO	PS/PS/NS	PS/PS/PS	PS/PS/PS	PS/PS/PS	PM/PS/PS	PB/ZO/PB
PB	PB/ZO/PB	PS/PS/PM	PS/PS/PM	PS/PS/PM	PS/PS/PS	PS/PS/PS	PB/ZO/PB

3. YAW moment distributor

3.1 Regular Distribution

The regular distribution scheme produces 1/2 of the required additional yaw moment on the front and rear axles, while ensuring that the sum of the four wheel independent drive torques is equal to the total target drive torque required by the driver. The specific allocation rules are as follows:

$$\Delta M_1 = \frac{B}{2}(T_{x1} - T_{x2}) \tag{4}$$

$$\Delta M_2 = \frac{B}{2}(T_{x3} - T_{x4}) \tag{5}$$

$$\Delta M_1 = \Delta M_2 = \frac{1}{2}\Delta M \tag{6}$$

$$T_{x1} + T_{x2} + T_{x3} + T_{x4} = T_D \tag{7}$$

Where, $T_{x1}, T_{x2}, T_{x3}, T_{x4}$ are the driving torques of each wheel; $\Delta M_1, \Delta M_2$ are the additional yaw moments distributed to the front and rear axles respectively.

3.2 Drive force distribution based on adhesion margin

The value of tire adhesion utilization represents the ability of providing adhesive force between the vehicle's tire and the pavement, with a maximum of 1, which characterizes the stability of the vehicle. According to the literature [20],The objective function of the optimal allocation is the sum of the four wheels' adhesion utilization rate, as shown below:

$$\min J = \sum_{i=fl,fr,rl,rr} \frac{{F_{xi}}^2 + {F_{yi}}^2}{(\mu_i F_{zi})^2} \tag{8}$$

The lateral force F_{yi} is taken as the boundary constraint of the objective function, and the control target for optimized allocation is the longitudinal force F_{xi} of four wheels.Assuming that the adhesion coefficient of each wheel on the same road is the same value; the above objective function can be finally transformed into:

$$\min J = \sum_{i=fl,fr,rl,rr} C_i \frac{{F_{xi}}^2}{(\mu_i F_{zi})^2} \tag{9}$$

Change the above formula into matrix form:

$$\min J_m = U^T W U \tag{10}$$

Where,$U = [F_{xi}]^T$,W is the weight coefficient of four−wheel longitudinal force, in the form of:

$$W = \begin{bmatrix} \frac{1}{(\mu F_{zfl})^2} & 0 & 0 & \\ 0 & \frac{1}{(\mu F_{zfr})^2} & 0 & 0 \\ 0 & 0 & \frac{1}{(\mu F_{rl})^2} & \\ & & & \frac{1}{(\mu F_{rr})^2} \end{bmatrix}$$

At this point, the objective function with the minimum sum of independent driving tire utilization is established.

3.3 Constraint boundary of driving torque distribution

In order to meet the driver's power control requirements for the vehicle, the sum of the driving torques of the four motors should be matched with the driver's total torque command, and the longitudinal force of the wheel should also satisfy the yaw moment relationship. The equation constraints are as follows:

$$F_{x\_desire} = (F_{xfl} + F_{xfr})\cos\delta + (F_{xrl} + F_{xrr}) \tag{11}$$

$$M_d = \frac{d}{2}(F_{xfl} - F_{xfr})\cos\delta + \frac{d}{2}(F_{xrl} - F_{xrr}) \tag{12}$$

Change the above formula into matrix form:

$$V = KU \tag{13}$$

Among them,$V = [F_{x\_desire}, M_d]^T$, $K = \begin{bmatrix} \cos\delta & \cos\delta & 1 & 1 \\ \frac{d}{2} & -\frac{d}{2} & \frac{d}{2} & -\frac{d}{2} \end{bmatrix}$.

Motor torque output value maximum limit:

$$-\mathrm{T_{maxi}} \le \mathrm{T_{xi}} \le \mathrm{T_{maxi}}, \mathrm{i} = \mathrm{fl, fr, rl, rr} \quad (14)$$

The relationship between wheel driving forceF_{xi} and hub motor torqueT_{xi} is as follows:

$$F_{xi} = \frac{T_{xi}}{r}, i = fr, fr, rl, rr \quad (15)$$

Substitute equation (15) into the equation (14) to get:

$$\frac{-\mathrm{T_{maxi}}}{\mathrm{r}} \le \mathrm{F_{xi}} \le \frac{\mathrm{T_{maxi}}}{\mathrm{r}}, \mathrm{i} = \mathrm{fl, fr, rl, rr} \quad (16)$$

The maximum adhesive force the ground can provide on the tire constraints:

$$0 \le \mathrm{F_{xi}} \le \sqrt{(\mu \mathrm{F_{zi}})^2 - \mathrm{F_{yi}}^2}, \mathrm{i} = \mathrm{fl, fr, rl, rr} \quad (17)$$

Overview, the objective function constraint condition of driving torque optimization was established, and the feasible solution constraint of the objective function was set under the above conditions to realize the optimal allocation scheme design of four-wheel drive torque constraint.

3.4 Objective function solving based on quadratic programming

Quadratic programming method can not only take into account many constraints of vehicle driving force, but also improve the efficiency of torque distribution controller. The quadratic programming method is used to solve the objective function. The general form is:

$$\min \mathrm{J} = \mathrm{U^T W U} + \mathrm{f^T U} \quad (18)$$

$$\mathrm{s.t.\ AU} \le \mathrm{b.\ A_{eq} U} = \mathrm{b_{eq}.\ LB} \le \mathrm{U} \le \mathrm{UB} \quad (19)$$

Combing the objective function and constraints, The quadratic coefficient matrix W and the primary coefficient matrix $\mathrm{f^T}$ can be obtained by the formula (12); $\mathrm{A_{eq}}$ and $\mathrm{b_{eq}}$ are equations of equality constraint coefficients, obtained by equation (13);A and b are inequality constraint coefficient matrices, Here are all zero matrices; LB and UB are upper and lower limits, which are obtained by the formulas (16) and (17).At this point,After the objective function and the constraint are converted into the quadratic programming standard form, the solution is the actual distribution torque of the four wheels, namely, the actual output of the yaw moment distributor.

4. Experimental verification

4.1 Simulation experiment

In order to verify the effectiveness of torque constraint allocation control strategy, compare it with the regular distribution with the Carsim-Simulink co-simulation verification. The simulink model is composed of four parts,

including the signal input layer composed of pedal and steering signal, the yaw moment decision layer based on yaw rate tracking control, the torque distribution layer taking the minimum tire utilization rate as the control target under multiple constraints, and the motor control stability layer controlling the four-wheel driving force. The adhesion coefficient of the dry road is set to u=0.85, and the adhesion coefficient of the wet road is set to u=0.3, which were selected for the comparative verification of driving stability control effect. The basic parameters of the simulation vehicle and in-wheel motor is presented in Table 2.

Table 2

Basic parameters of simulationvehicle

Parametername	Value	parameter name	value
Vehicle mass /kg	1111	vehicle height /mm	1780
Height of center of mass/mm	540	Moment of inertia around the x-axis /kg·m2	288
Moment of inertia around the z-axis /kg·m2	2031.4	Moment of inertia around the y-axis /kg·m2	2031.4
Wheel base/mm	2600	Width/mm	1440
Distance from centroid to front axle /mm	1040	Front axle lateral stiffness /N·rad-1	-53388
Distance from centroid to rear axle /mm	1560	Rear axle lateral stiffness/N·rad-1	-35592
Front wheel radius /mm	311	Rear wheel radius /mm	311
Rated power(kW)	3	Rated voltage (V)	72
Maximum speed(rpm)	700	Maximum torque(Nm)	161

1) Simulation experiment of high and low adhesion pavement with double lane change

Set the road adhesion coefficient u=0.85, and the driver's target speed is 100Km/h. It can be seen from Figure.3(a),(b) that, compared with the regular distribution, the tracking of yaw rate and lateral deflection of the center of mass under torque constraint distribution is faster, and less overshot. As can be seen from Figure.3(c), when the vehicle is steered, the vertical load of the inner wheel is smaller than that of the outer wheel. To prevent the vehicle from slipping and under steering, the inner wheel driving force should be reduced and the outer driving force increased.Also, Fig.3(d) shows that torque constraint distribution distributes torque between front and rear wheels on the same side of the vehicle, enabling the steering process to makefull use of the grip of tires and realize the stability control of vehicles under high-adhesion road surface.

Set the road adhesion coefficient u=0.3 and target speed is 100Km/h. In Fig.3(e),(f), the torque constrained yaw rate curve overshoot is smaller than the regular distribution scheme, and the follow-up effect on the driver's steering wheel

input is more ideal, It can make full use of the tire adhesion rate to distribute the four-wheel torque, so the yaw control effect is relatively stable. From Figure.3(g), (h), the torque constraint distribution provides a greater driving force for tires with a larger vertical load in the steering process, while reducing the driving force for wheels with a smaller vertical load. In Fig. 3, the legend information is: FR - front right wheel, FL - front left wheel, RL - rear left wheel, RR - rear right wheel.

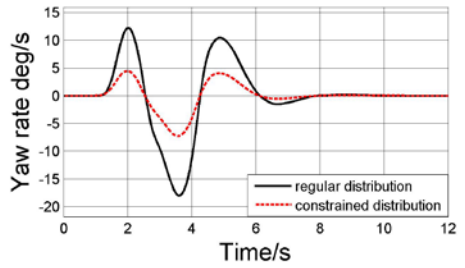

(a) Yaw rate

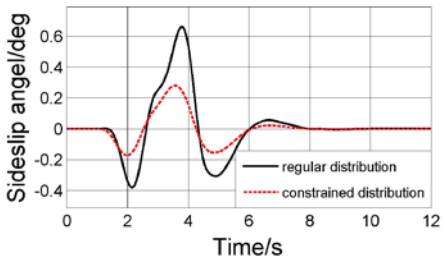

(b) Sideslip angle

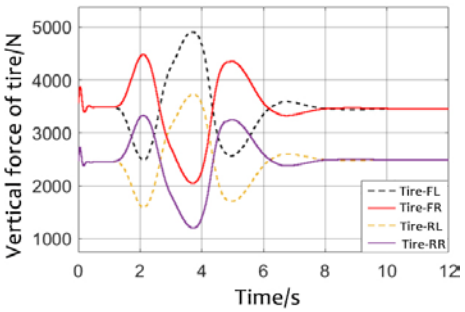

(c) Vertical force of tire

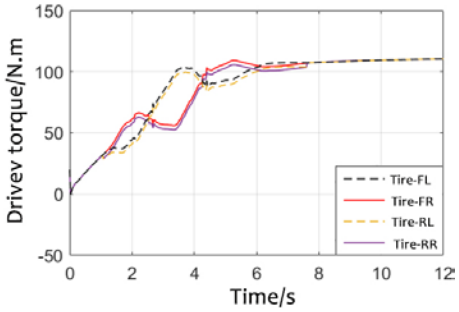

(d) Drive torque

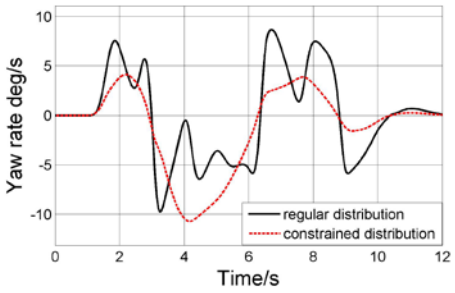

(e)Yaw rate

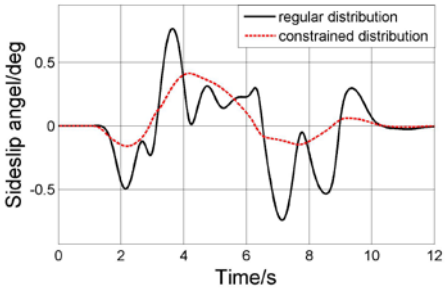

(f) Sideslip angle

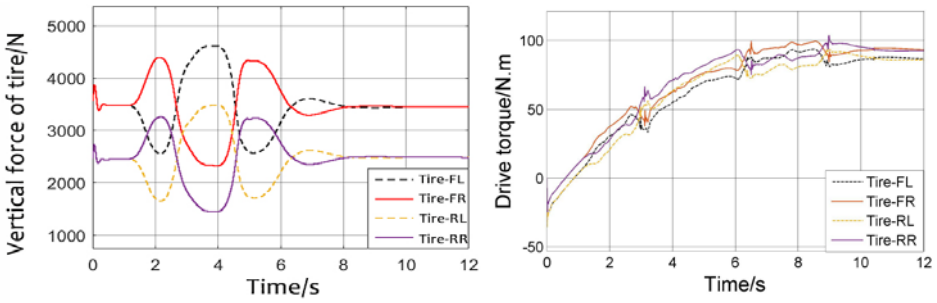

(g) Vertical force of tire (h) Drive torque

Fig. 3. Vehicle state parameters under double lane change simulation

1) **Simulation experiment of high and low adhesion pavement under serpentine condition**

Set the road adhesion coefficient u=0.85 and the driver's target speed is 100Km/h. As shown in Fig.4(a),(b), the torque constraint distribution is implemented on the vehicle stability control and trajectory tracking. The control effect is slightly obvious than the torque rule distribution, and the curve control effect is more gradual. According to Fig.4(c), (d), in the running process, the wheel with a larger load is distributed to a larger driving torque, and vice versa.

Set the road adhesion coefficient u=0.3 and the target vehicle speed is 100Km/h. According to Fig.4(e),(f), the torque constraint distribution is superior to the general distribution for the control of yaw rate and sideslip angle. According to Fig.4(g),(h), the distribution mode of driving torque can still be distributed according to the vertical load distribution, making full use of the adhesion rate of tires.

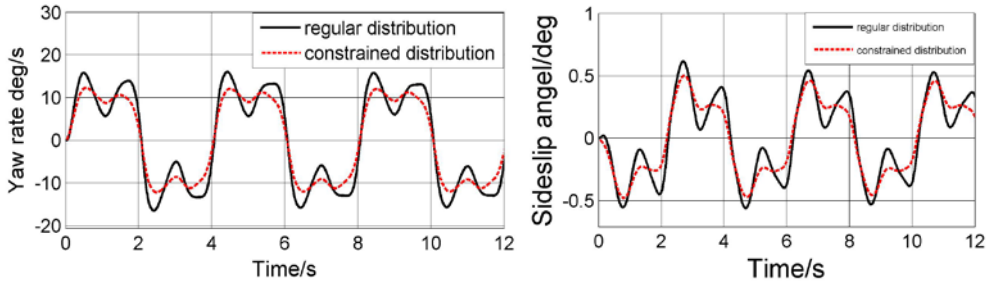

(a) Yaw rate (b) Sideslip angle

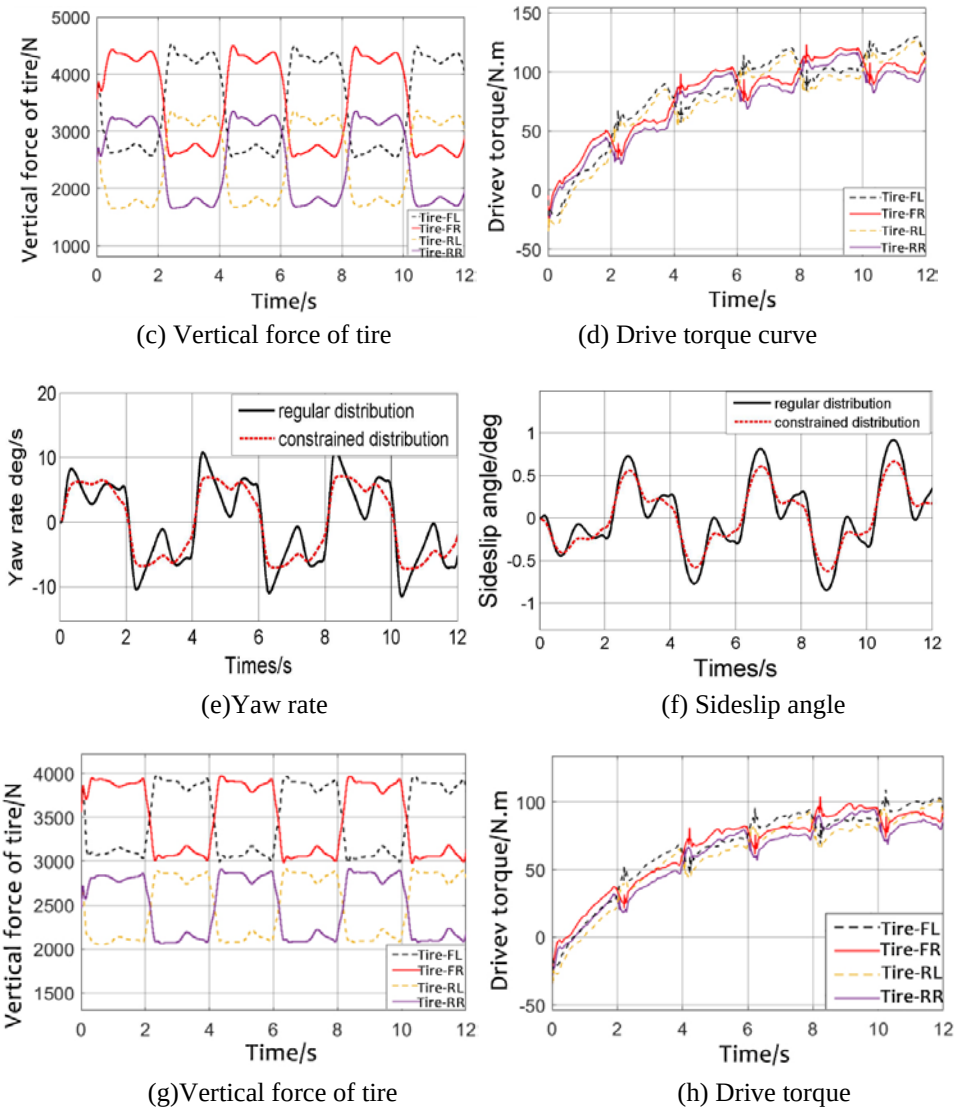

(c) Vertical force of tire (d) Drive torque curve

(e)Yaw rate (f) Sideslip angle

(g)Vertical force of tire (h) Drive torque

Fig. 4. Vehicle state parameters under serpentine simulation

4.2 Hardware in loop experiment

This paper is based on dSPACE((1401/1513/1514)) for HIL experiments. The dSPACE processor collects the data of EFP along with the steering angel sensor in real-time and meanwhile feeds back the signal to the CarSim vehicle model. CarSim genearates a virtual scene projected to a large screen,according to which the driver perceives the driving environment and operates the vehicle. The experimental platform is shown in Fig..5 blow. Angle sensor adopts SX-4300. It is LH3 steering sensor with torque angle of ±8°, multi-turn position effective angle

of ±720°, angle signal accuracy is ±3%. EFP uses the ipPD-12V Inbol Hall-type electronic throttle, the supply voltage is 12V, output signal is 0V~4.7V±0.1V. After completing the verification of co-simulation platform, parameters of RTW(real-time Workshop) are configured to automatically generate c code to realize the model function, and the RTI(real-time interface) can be directly accessed and configured. Through RTI compilation, the target code is generated and downloaded to dSPACE for the HIL experiment.

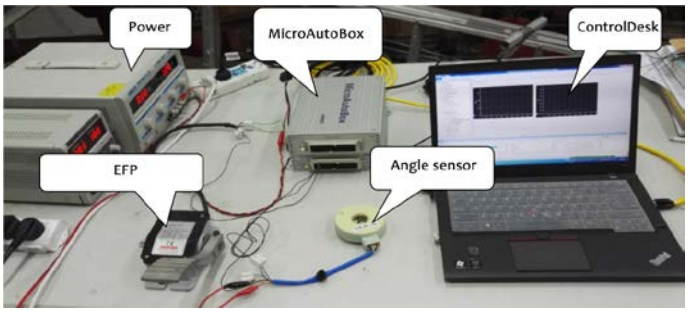

Fig. 5. Experimental platform

1) Double lane change condition

In order to highlight the control effect of torque constraint distribution, the high-adhesion road surface is selected; target vehicle speed is set to100Km/h. The input signal of the steering wheel is shown in Fig. 6(a) below. Ignoring the vibration and deviation of the input steering wheel signal, it can be seen from Figure.6(b),(c) that the control effect of the yaw rate and the sideslip angle is basically consistent with the co-simulation. The yaw moment controller can realize the tracking of the yaw rate under the change of the steering input. As shown in Figure.6(d), when the steering wheel signal input is zero, the vehicle runs in a straight line, and the driving force distributed by the four wheels remains the same. In the case of steering, the wheels with larger vertical load are distributed with more driving force to make the steering process more stable.

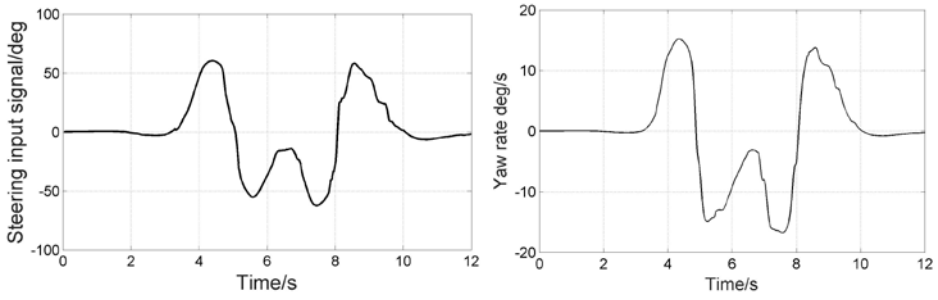

(a) Steering angle input signal (b)Yaw rate

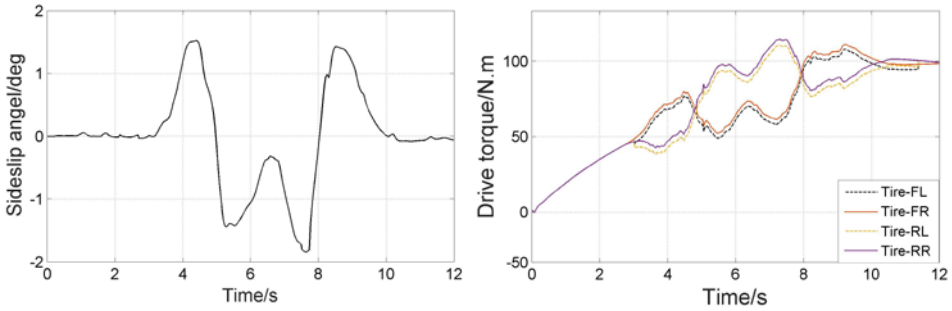

(c) Sideslip angle (d) Drive torque in constrain distribution

Fig. 6. Vehicle state parameters under double lane change hardware-in-loop simulation

2) Serpentine condition

In the serpentine road condition, the vehicle will complete continuous driving in a variable direction. The high-adhesion road surface is selected for the experimental road surface, and the target speed is 100Km/h. Steering wheel signals of serpentine road conditions are shown in Figure.7 (a) below.

Ignoring the vibration and deviation of the input steering wheel signal during the experiment, Fig.7(b),(c) show that the serpentine road conditions, yaw rate and the sideslip angle have some fluctuations, but in actual driving process, its values are within a reasonable scope, the control effect of yaw rate and sideslip angle is basically consistent with simulation, on this occasion, the following effect of steering wheel signal is good, the results prove that drive control strategy under the working condition of serpentine can still achieve drive stability of vehicle control. According to Figure.7 (d), in the turning process, the hub motor provides different driving torques to the four wheels. On the basis of the different distribution of vertical load among the four wheels, the reasonable driving torques is distributed to finally realize the stability control in serpentine conditions.

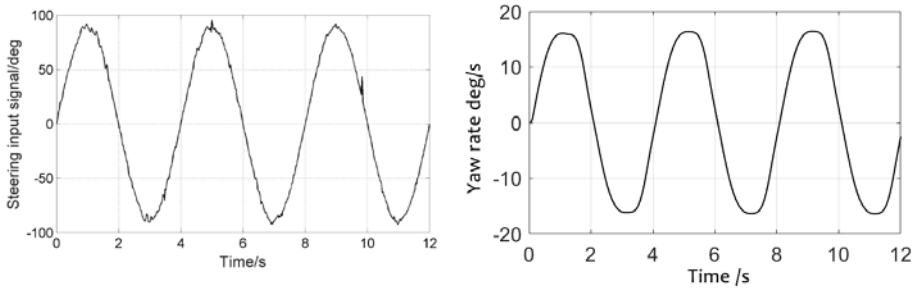

(a) Steering angle input signal (b) Yaw rate

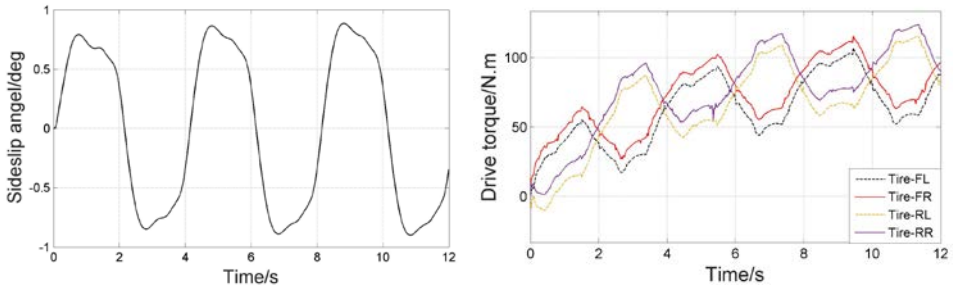

(c)Sideslip angle (d)Drive torque in constrain distribution

Fig.7. Vehicle state parameters under serpentine hardware-in-loop simulation

5. Conclusion

1) The upper fuzzy PID control algorithm of the controller is concise and practical. The vehicle target motion state parameters can be well tracked. The optimal allocation algorithm of lower yawing moment controller can not only ensure the DYC control effect of the vehicle, but also reduce the utilization rate of tire adhesion and increase the potential of stable operation of the vehicle.

2) Simulation experiments and semi-physical experiments were carried out with Carsim/Simulink and dSPACE under double-lane change condition and serpentine condition. The proposed strategy, compared with general distribution, simulation results showed that torque optimization allocation is more rapid and accurate in tracking vehicle state parameters; dSPACE is used for semi-physical simulation verification, and the experimental results are in line with the simulation results, which is applicable to the range of vehicle motion state and beneficial to the real vehicle application.

Acknowledgement

This work was funded by the foundation of Shaanxi Key Laboratory of Integrated and Intelligent Navigation grant number SKLIIN-20180101.

R E F E R E N C E S

[1]. *Huan-Huan, Zhang , X. Xu-Ai , and Y. E. Ke-Bao.* Research of Torque Allocation Strategy of Four-wheel Independent Driving Electric Vehicle Based on Stability.Journal of Highway and Transportation Research and Development, 11.1(2017):98-102..

[2]. *Chen, B. C., and C. C. Kuo.* Electronic stability control for electric vehicle with four in-wheel motors.International Journal of Automotive Technology 15.4(2014):573-580.

[3]. *Shino, Motoki, and M. Nagai.* Yaw-moment control of electric vehicle for improving handling and stability. Jsae Review, 22.4(2001):473-480.

[4]. *Hu, Jia Sheng et al.* Robust Yaw Stability Control for In-wheel Motor Electric Vehicles.IEEE/ASME Transactions on Mechatronics, (2017):1-1.
[5]. *Xinbo, Ma, et al.* Cornering stability control for vehicles with active front steering system using T-S fuzzy based sliding mode control strategy. Mechanical Systems and Signal Processing, (2018):S0888327018303182-.
[6]. *Tahami, Farzad, S. Farhangi, and R. Kazemi*. A Fuzzy Logic Direct Yaw-Moment Control System for All-Wheel-Drive Electric Vehicles. Vehicle System Dynamics, 41.3(2004): 203-221.
[7]. *Jinghua, Guo, L. Yugong, and L. Keqiang.* Adaptive non-linear trajectory tracking control for lane change of autonomous four-wheel independently drive electric vehicles. IET Intelligent Transport Systems, 12.7(2018):712-720.
[8]. *Ding, X., et al.* Integrated DYC/ASR-based variable universe fuzzy control for electric vehicles. Qiche Gongcheng/Automotive Engineering, 36.5(2014):527-531+545.
[9]. *Raksincharoensak, Pongsathorn, M. Nagai , and M. Shino.* Lane keeping control strategy with direct yaw moment control input by considering dynamics of electric vehicle. Vehicle System Dynamics 44.sup1(2006):192-201.
[10]. *Yu, Zhuoping, et al.* Direct yaw moment control for distributed drive electric vehicle handling performance improvement." Chinese Journal of Mechanical Engineering, 29.3(2016):486-497.
[11]. *Clarke,D.W.*GeneralizedPredictiveControl-PartII.ExtensionsandInterpretations.Automatica, 23.2(1987):137-148.
[12]. *Dai, Yifan , et al.* Optimum tyre force distribution for four-wheel-independent drive electric vehicle with active front steering. International Journal of Vehicle Design 65.4(2014):336.
[13]. *Wang, Zhenpo, et al.* Optimal Component Sizing of a Four-wheel Independently-Actuated Electric Vehicle with a Real-time Torque Distribution Strategy. IEEE Access PP.99 (2018):1-1.
[14]. *YANIV, and ODED.* Robustness to Speed of 4WS Vehicles for Yaw and Lateral Dynamics. Vehicle System Dynamics, 27.4(1997): 221-234.
[15]. *Li, Gang, and Z. Yang.* Energy saving control based on motor efficiency map for electric vehicles with four-wheel independently driven in-wheel motors. Advances in Mechanical Engineering, 10.8(2018):168781401879306-.
[16]. *Xu Dan, Wang Guodong,Cao Binggang,etc.*Study on optimizing torque distribution strategy for independent 4WD electric vehicle. Hsi-An Chiao Tung Ta Hsueh/Journal of Xi'an Jiaotong University,46(3): 42-46,68.2012
[17]. *Lian, Y. F., et al.* Direct Yaw-moment Robust Control for Electric Vehicles Based on Simplified Lateral Tire Dynamic Models and Vehicle Model. IFAC-PapersOnLine 48.28(2015):33-38.
[18]. *Kobayashi, Takao, et al.* Efficient direct yaw moment control: tyre slip power loss minimisation for four-independent wheel drive vehicle.Vehicle System Dynamics, 56.5(2018):1-15.
[19]. *YU Zhisheng.* automobile theory. Beijing: China Machine Press, 2009.
[20]. *Mokhiamar, Ossama , and M. Abe.* Simultaneous Optimal Distribution of Lateral and Longitudinal Tire Forces for the Model Following Control. Journal of Dynamic Systems Measurement and Control, 126.4 (2004):753-763.